Mn-site hyperfine fields in $LaMnO_3$ and $NdMnO_3$ measured using perturbed-angular-correlation spectroscopy

Robert L. Rasera
Department of Physics, University of Maryland Baltimore County, Baltimore, Maryland 21250

Gary L. Catchen
Department of Nuclear Engineering, The Pennsylvania State University, University Park, Pennsylvania 16082
(Received 3 February 1998; revised manuscript received 26 March 1998)

Using perturbed-angular-correlation spectroscopy, we have measured the temperature dependence of hyperfine interactions at ^{181}Ta nuclei at Mn sites in ceramic samples of nominally stoichiometric $LaMnO_3$ and $NdMnO_3$. Magnetic hyperfine fields (MHF's) and electric-field gradients (EFG's) were measured from 10 to 296 K. The perturbation functions measured for both compounds show sharp line shapes, indicating low defect populations in the vicinity of the probe ions. The Mn-site EFG's show a weak dependence on temperature in both compounds, and the associated quadrupole frequencies and EFG asymmetries are very large. At laboratory temperature, $\omega_Q = 158.3(2)$ Mrad s^{-1} and $\eta = 0.82(1)$ for $LaMnO_3$, and $\omega_Q = 190.9(3)$ Mrad s^{-1} and $\eta = 0.80(2)$ for $NdMnO_3$. Below the respective magnetic ordering temperatures of 138 and 85 K for the La and Nd compounds, the dependence on reduced temperature of the observed supertransferred MHF's follows a power law, with an exponent of 0.41(1) in each case. The analysis of the combined magnetic-dipole and electric-quadrupole interaction yields the angle β between the principal z axis of the EFG tensor and the direction of the MHF, which is 56.5(5)° at 10 K for $LaMnO_3$ and 62.5(5)° at 10 K for $NdMnO_3$. For $LaMnO_3$, the angle β shows negligible temperature dependence, whereas for $NdMnO_3$ this angle decreases linearly with increasing temperature. [S0163-1829(98)04230-1]

I. INTRODUCTION

Rare-earth perovskite compounds such as $LaMnO_3$ provide a basis from which technologically important materials may be developed. When doped with alkaline-earth elements in the rare-earth site, thin films of these compounds exhibit unusual electric and magnetic properties such as ''colossal magnetoresistance.'' [1] These highly distorted crystals have complex phase diagrams, and show various types of magnetic ordering that depend sensitively on the presence of dopants and defects. Perturbed-angular-correlation (PAC) spectroscopy is a technique that provides information on the magnetic ordering and related properties of these compounds. PAC senses the local electromagnetic environment of radioactive probe atoms substituted into specific sites in a crystal by observing the magnetic hyperfine fields (MHF's) and electric-field gradients (EFG's) generated by the electrons and nuclei that surround them.[2] The interactions of the probe nucleus' magnetic-dipole and electric-quadrupole moments with the extranuclear MHF and EFG, respectively, perturb the spatial and temporal correlations of the γ rays emitted by the ^{181}Ta excited nuclei after the radioactive decay of ^{181}Hf occurs. Because the PAC technique is very sensitive to changes in the local probe environment, the technique can provide both static and dynamic information about the effects of dopants and defects that change the local EFG. This is manifest in the broadening and attenuation of the measured line shapes.

In magnetically ordered perovskite crystals, the magnetic-dipole interaction arises at the site of the nonmagnetic probe ions through the transfer of spin density from the magnetic ions (in the present case, Mn) through O p orbitals to valence orbitals of the probe ion, where the ''supertransferred magnetic hyperfine field'' [3] (STHF) polarizes the probe nucleus. This effect is extremely sensitive to the spatial extent of the atomic wave functions. For this reason, measurements of these fields provide information that stringently tests structural theory.

As a first step, we have carried out PAC measurements on the parent compounds, i.e., nondoped samples, in order to establish a baseline with which to compare the behavior of doped compounds that show effects such as colossal magnetoresistance. We selected two parent compounds that have similar crystal structures but have very different crystal chemistry. For ceramics of the $LaMnO_3$ compound, the Mn^{4+} ion concentration can range from negligibly small to several tens of percent, and cation vacancies provide the primary electrical compensation for the excess charge of the Mn^{4+} ions.[4] The Mn^{4+}-ion concentration depends strongly on processing conditions, and it determines the low-temperature crystal structure.[4,5] For ceramics of the $NdMnO_3$ compound, in contrast, Mn-ion-produced deviations from stoichiometry are relatively small.[4] Thus, we expect ceramic samples of $LaMnO_3$ to contain measurable quantities of Mn^{4+} ions, and ceramic samples of $NdMnO_3$ to contain insignificant amounts of these ions. Therefore, by comparing the measured line shapes for the two compounds, we can determine the extent to which differences in the Mn^{4+}-ion concentration affect the hyperfine fields at the ^{181}Ta probe. Because doping and the associated production of defects modify the electric and magnetic properties of these crystals, this line-shape information provides the necessary bench-

mark to which PAC measurements on highly doped derivatives of these parent compounds can be compared. In this case we expect substantial line broadening caused by random distributions of cations and defects. We have made preliminary exploratory measurements that confirm this expectation. Since the line shapes for the parent compounds do not show large amounts of line broadening, the analysis of these sharp lines therefore offers potentially the most precise and detailed information about the MHF's at the Mn sites in these compounds.

II. EXPERIMENTAL METHODS

Ceramic samples of $LaMnO_3$ and $NdMnO_3$ were prepared using a resin-intermediate method, involving the metal precursors $La(OH)_3$, $Nd(NO_3)_3$, and $Mn(CH_3COO)_3$. A $HfOCl_2$ solution carrying the ^{181}Hf activity was added to the resin-forming mixture. The Hf concentration in the products was $\approx$0.07 at. % of the Mn concentration. The resulting powder of mixed oxides was pressed into small pellets and sintered at 1770 K for 15–30 min under flowing Ar gas. This reducing atmosphere favors production of stoichiometric ceramics in which the Mn ions are primarily in the 3+ oxidation state. The samples were crushed after sintering and sealed into small fused-silica tubes. X-ray-diffraction patterns show the radioactive powder samples to be phase pure within a few percent. Huang *et al.* have carried out a careful investigation of the phase composition of stoichiometric $LaMnO_3$.[6] They find that processing $LaMnO_3$ under the foregoing conditions leads to the production of a phase that orders antiferromagnetically at low temperatures.

The question arises as to which site the ^{181}Hf probe parent occupies in the crystal. The charge state (4+) and the radius (0.85 Å) of the probe ion provide little guidance. However, the MHF's that we observe at the probes are large, i.e., several tens of kOe, and the transfer of spin density in the perovskite structure is only favorable when the metal-ion-oxygen–metal-ion bond angle approaches 180°.[7] Specifically, for the lanthanide-manganese-oxygen perovskites, the Mn-O-Mn bond angle approaches 180°, and the Ln-O-Mn bond angle approaches 90° (Ln represents the lanthanide.) If the probe ion were to substitute into the Ln sites, very little spin density would be transferred from the nearest Mn ions to the probe ion's outer *s* orbitals, because this bond angle corresponds to a very small overlap of oxygen *p* orbitals with 4*s* and 5*s* orbitals of the probe. Thus, the MHF at the probe-ion nucleus would be very small. However, if the probe ion substitutes into the Mn sites, a large spin density would be transferred to the probe-ion orbitals, giving rise to a very large MHF at the probe-ion nucleus. The measured MHF's, as well as those measured at the *B* sites in other ABO_3 perovskites using PAC spectroscopy,[3,8,9] are consistent with this latter model. Therefore, we assign the probe site substitution to the Mn site in both $LaMnO_3$ and $NdMnO_3$.

The PAC time distributions were measured using a three-BaF_2-detector spectrometer, which has a time resolution of 700 ps full width at half maximum for the 133–482 keV γ cascade in ^{181}Ta. A closed-cycle helium refrigerator was used to cool the samples. The temperature was electronically stabilized to within $\pm$0.1 K over the duration of a measurement. For a polycrystalline sample, the measured angular correlation function $W(\theta,t) = \exp(-t/\tau_N)\Sigma_k A_{kk} G_k(t) P_k(\cos\theta)$, where θ and t are the angle between emission directions of the cascade γ rays, and the time between emission of the first and second γ rays, respectively. τ_N and A_{kk} are nuclear parameters, and the extranuclear hyperfine interaction is represented by the perturbation factor $G_{kk}(t) = \Sigma_i s_i \cos(\omega_i t)\exp(-\delta\omega_i t)$, where the parameter δ is a measure of the width of the Lorentzian distribution of the hyperfine frequencies about their mean values. The frequencies ω_i and their amplitudes s_i are related to the hyperfine splitting of the intermediate nuclear level. Above T_N, where no MHF is present, three interaction frequencies ω_i are observable, related to the electric-quadrupole interaction (EQI) frequency $\omega_Q = eQV_{zz}/4I(2I-1)/\hbar$ and the asymmetry parameter $\eta = (V_{xx} - V_{yy})/V_{zz}$, where the V_{ii} are the elements of the EFG tensor in its principal axis system. Below T_N, the ω_i are obtained by diagonalizing the hyperfine interaction matrix resulting from the combination of the EQI with the MHF represented by the magnetic frequency $\omega_B = -g_I\mu_N B/\hbar$. The EFG coordinate system is taken to be oriented at an Euler angle set (0, β, γ) with respect to the direction of the MHF.[10] Because of the lifting of the degeneracy of the EQI by the addition of the MHF, the number of allowable ω_i is increased from three to (in principle) 15.[11] However, in the present case, the combined effects of large EFG asymmetry, limited time resolution, and energy-state degeneracies reduce the number of resolvable frequencies to six. The hyperfine parameters were extracted from the measured perturbation functions using the DEPACK program developed by Lindgren.[12]

III. RESULTS

Figures 1 and 2 present two perturbation functions and the corresponding squared Fourier transforms measured in $LaMnO_3$ and $NdMnO_3$, respectively, above and below the magnetic ordering temperature T_N. At temperatures above T_N, the Fourier transforms show three well-defined peaks, whereas below T_N six peaks can be resolved, which reflects the limitation of time resolution. For both compounds, the perturbation functions measured above the magnetic ordering temperature show sharp lines ($\delta = 0.024$ to 0.030 for $LaMnO_3$ and $\delta = 0.015$ to 0.030 for $NdMnO_3$, depending on sample) that characterize a very strong and highly asymmetric EFG. The small amount of line broadening indicates that the probe environments in both samples are relatively free of point defects. Because the nominal charge of the parent Hf probe ion is 4+ in these compounds, electrostatic energy considerations make it likely that relatively few Mn^{4+} ions occur in the near vicinity of the probe. Thus, the sharp lines, which are associated with this low local defect concentration, enable us to accurately measure the interaction frequencies that correspond to the combined nuclear magnetic-dipole and electric-quadrupole interaction, which characterize the perturbation functions measured below T_N. For these below-T_N perturbation functions, we can determine the parameters ω_Q, ω_B, η, and δ, and the Euler angle β, although the measurements are relatively insensitive to the angle γ. If we were to observe a large amount of line broadening, which would accompany, for example, Ca doping at 20 at. %, we would not be able to accurately determine all of these parameters. Per-

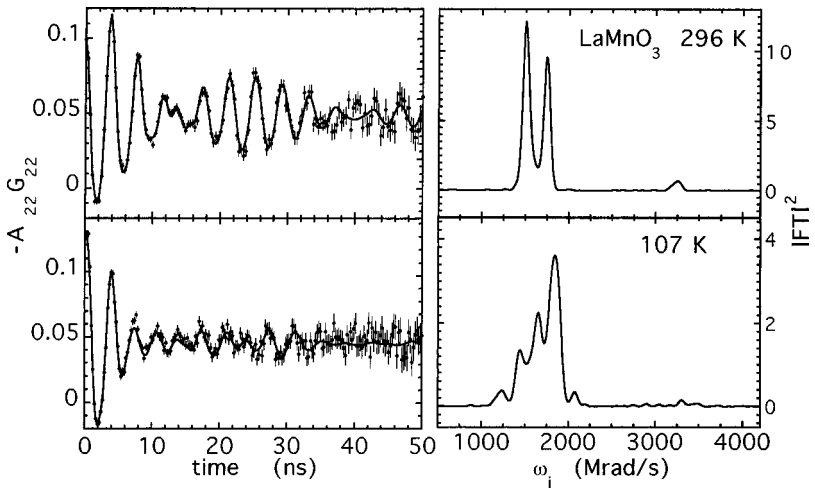

FIG. 1. Representative measured perturbation functions and their squared Fourier transforms for $LaMnO_3$, at temperatures above T_N (upper set) and below T_N (lower set).

haps only ω_B and δ could be independently resolved at temperatures below T_N. Therefore, these measurements represent a very accurate characterization of the Mn-site hyperfine fields in these two parent compounds.

Figure 3 summarizes the temperature dependences of the electric-quadrupole interactions from 10 K to laboratory temperature. For both compounds, the quadrupole frequency ω_Q and the associated asymmetry parameter η show a weak dependence on temperature. For $LaMnO_3$, ω_Q decreases slowly with increasing temperature, while for $NdMnO_3$, ω_Q remains relatively constant, consistent with the lattice expansion expected in perovskites. By contrast, the asymmetry parameter η for both compounds increases somewhat with increasing temperature, indicating that the local site symmetry becomes lower as temperature increases. This result is counter to the usual behavior of perovskite crystals, which generally become more symmetric at higher temperature.[13]

IV. DISCUSSION

For the measurements below T_N, Figs. 4 and 5 summarize the derived parameter values for $LaMnO_3$ and $NdMnO_3$, respectively. The temperature dependence of the MHF as represented by the measured magnetic frequencies ω_B can be accurately represented by a power law: $\omega_B(T)=\omega_B(0)[1-T/T_N]^{\beta}$. For the La and Nd compounds, the extrapolated magnitudes of the magnetic frequencies at 0 K are 215(2) Mrad s^{-1} and 177(1) Mrad s^{-1}, respectively, corresponding to zero-temperature MHF's of 34.8(3) kOe for $LaMnO_3$ and 28.6(2) kOe for $NdMnO_3$. The derived exponents β have values of 0.41(1) for both $LaMnO_3$ and $NdMnO_3$, which are consistent with exponents measured on other magnetic perovskites[8,14] and predicted from theory for three-dimensional magnetically-ordered crystals.[15] These exponent values differ from the value of 0.26(1) derived from neutron scattering measurements on nominally stoichiometric samples of $LaMnO_3$.[16] For this large and unexpected difference, we can at the moment offer no detailed explanation. However, we emphasize that the PAC-measured MHF's have a fundamentally different physical origin than the order parameter measured in neutron scattering.[16] Neutron scattering measures the average effect of the exchange interaction on the magnetic ordering correlated over large distances in the crystal; whereas, the PAC-measured MHF's arise, because spin density is transferred from magnetically-ordered Mn d orbitals through O p orbitals into primarily 4s and 5s orbitals of the ^{181}Ta probe ion. The polarization of the probe nucleus by the transferred spin density gives rise to the observed perturbation of the angular correlation, to which correspond the measured ''supertransferred'' MHF's. Both neutron scattering and PAC measure the exchange interaction indirectly and from different vantage points.

As mentioned above, we expect that nominally stoichio-

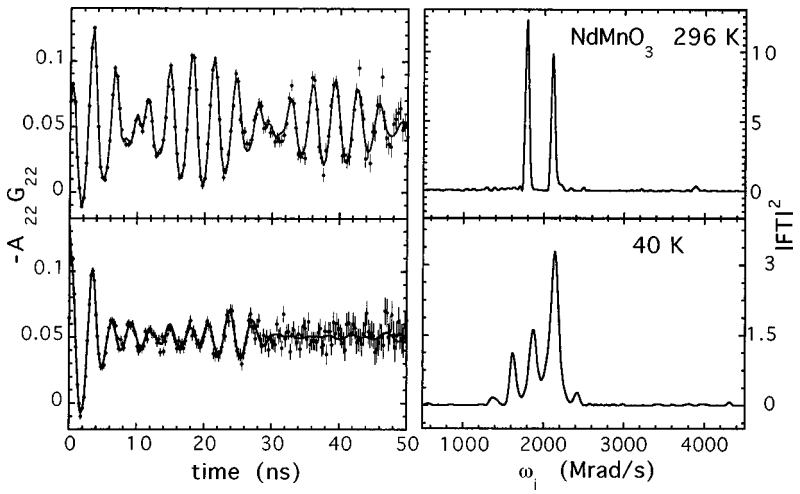

FIG. 2. Representative measured perturbation functions and their squared Fourier transforms for $NdMnO_3$, at temperatures above T_N (upper set) and below T_N (lower set).

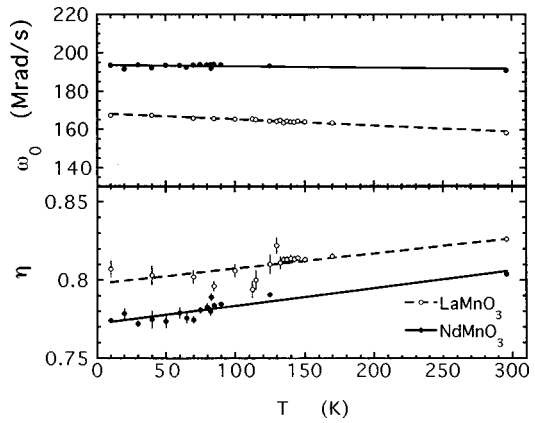

FIG. 3. Temperature dependence of the electric-quadrupole interaction parameters for $LaMnO_3$ (open circles) and $NdMnO_3$ (solid circles).

metric $LaMnO_3$ samples contain small but significant concentrations of Mn^{4+} ions, which could affect the magnetic ordering, whereas we expect the Mn^{4+} concentration to be negligible in $NdMnO_3$. The line shapes we measured in both compounds show comparable sharpness, and the associated power-law exponents have approximately the same value. These results suggest that, within the local environments of the ^{181}Ta probe ions, the local Mn^{4+} concentration is lower than the average concentration within the sample. Thus, PAC-measured MHF's may not sense the perturbation of the exchange interaction that small concentrations of Mn^{4+} ions would produce. This suggestion implies that the PAC measurements do not probe the exact equilibrium state of the $LaMnO_3$ crystal, in which the Mn^{4+} concentration would be the same in the vicinity of the probe as elsewhere in the crystal. This possibility reflects a limitation associated with our current experimental capability. In principle, $LaMnO_3$ samples could be prepared by more precisely controlling the oxygen partial pressure during sintering. This control would

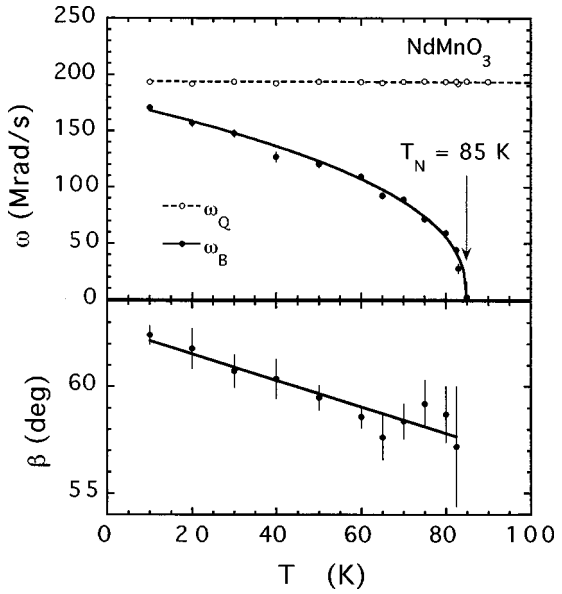

FIG. 4. Temperature dependence of the electric and magnetic hyperfine frequencies, and the angle between the MHF and the z axis of the principal axis system, for $LaMnO_3$ below T_N.

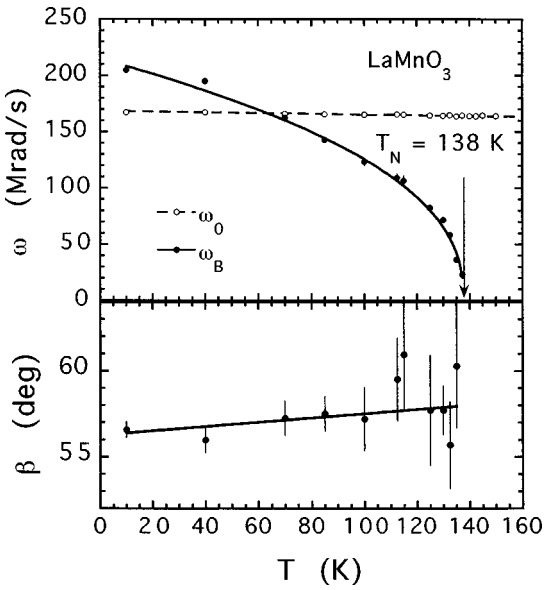

FIG. 5. Temperature dependence of the electric and magnetic hyperfine frequencies, and the angle between the MHF and the z axis of the principal axis system, for $NdMnO_3$ below T_N.

allow us to vary the gross Mn^{4+} concentration systematically and thereby investigate the dependence of the hyperfine interaction on the global Mn^{4+} concentration.

The angle β (distinct from the exponent β just discussed), which represents the angle between the principal z axis of the EFG and the direction of the MHF, shows no significant temperature dependence for $LaMnO_3$, but does show a substantial decrease with increasing temperature for $NdMnO_3$. This difference in the temperature dependence of the angle β suggests that the magnetic ordering in $NdMnO_3$ differs in detail from that in $LaMnO_3$. The relative constancy of the EFG parameters with temperature in $NdMnO_3$ indicates that it is the direction of the MHF that changes with temperature.

Although the basic perovskite lattice is relatively symmetric, we observe a large and asymmetric EFG in both materials. The point symmetry at the Mn site depends on the arrangement of its near neighbors, which are O ions in octahedra canted with respect to the major symmetry axes.[6] Consequently, the relationship between the directions of the principal axes of the EFG tensor and the major crystallographic axes is not obvious or easily calculable. If we were able *a priori* to determine the directions of the EFG principal axes with respect to the crystallographic axes, then we could determine, via the angle β, the direction of the MHF. This magnetic field represents the average effect of the transfer of spin density through the six Mn-O bonds, which are directed along the apices of the oxygen octahedra. If, for example, the Mn d electrons at the vertical apices were to order along the c direction and the Mn d electrons at the horizontal apices were to order along a direction in the a-b planes of the crystal, we would expect the magnitude and direction of the measured STHF to differ from that resulting from Mn d-electron spins that would be ordered in the same direction.

An alternative approach is to assume that the direction of the MHF lies parallel to the direction of the bulk-crystal magnetization. This assumption fixes the direction of the principal axis of the EFG tensor with respect to the crystal-

lographic axes. But to test this hypothesis more experiments are needed. For example, by changing the charge state of some of the Mn^{3+}-ions to 4+, the magnetic ordering can be changed from antiferromagnetic to ferromagnetic.

V. CONCLUSIONS

In conclusion, we have demonstrated that combined magnetic-dipole and electric-quadrupole interactions can be accurately measured in ^{181}Ta impurities at Mn sites in well-characterized ceramic samples of $LaMnO_3$ and $NdMnO_3$. The measured hyperfine interactions for both compounds exhibit similar qualitative features: (1) the EFG's are large and asymmetric; (2) the EFG asymmetries and the corresponding temperature dependences are anomalous; (3) the ratio of ω_B to ω_Q is of order unity; (4) the directions of the MHF's with respect to the principal z axes of the EFG's in both compounds are similar; (5) the temperature dependences of the MHF's show power-law behavior that is expected for three-dimensionally-ordered ferromagnets; and (6) the direction of the MHF appears to change with temperature in $NdMnO_3$ but not in $LaMnO_3$. Since the samples are nondoped stoichiometric compounds, these parameters provide a useful reference point for theoretical calculations and further experiments on doped manganates.

ACKNOWLEDGMENTS

We are grateful to Dr. B. Lindgren for his assistance in implementing his DEPACK PAC data analysis system. One of us (G.L.C.) wishes to acknowledge the hospitality of the Fakultät für Physik der Universität Konstanz, Germany. We thank Professor J. W. Lynn both for useful discussions and for communicating his results to us prior to publication. This work was supported in its initial stages by the Office of Naval Research under Grant No. N0014-90-J-4112.

[1] S. Jin, M. McCormack, T. H. Tiefel, and R. Ramesh, J. Appl. Phys. **76**, 6929 (1994).
[2] G. L. Catchen, J. Mater. Educ. **12**, 253 (1990); Mater. Res. Bull. **20**, 37 (1995).
[3] H. H. Rinneberg and D. A. Shirley, Phys. Rev. Lett. **22**, 1147 (1973); Phys. Rev. B **13**, 2138 (1976).
[4] G. J. McCarthy, P. V. Gallagher, and C. Sipe, Mater. Res. Bull. **8**, 1277 (1973).
[5] E. O. Wollan and W. C. Koehler, Phys. Rev. **100**, 545 (1995); W. C. Koehler and E. O. Wollan, J. Phys. Chem. Solids **2**, 100 (1957); A. Wold and R. J. Arnott, *ibid.* **9**, 176 (1958); G. Matsumoto, J. Phys. Soc. Jpn. **29**, 606 (1970); B. C. Tolfield and W. R. Scott, J. Solid State Chem. **10**, 183 (1974).
[6] Q. Huang, A. Santoro, J. W. Lynn, R. W. Erwin, J. A. Borchers, J. L. Peng, and R. L. Greene, Phys. Rev. B **55**, 14 987 (1997).
[7] C. Boekema, F. Van der Woude, and G. A. Sawatzky, Int. J. Magn. **3**, 341 (1972).
[8] T. M. Rearick, G. L. Catchen, and J. M. Adams, Phys. Rev. B **48**, 224 (1993).
[9] G. L. Catchen, T. M. Rearick, and D. G. Schlom, Phys. Rev. B **49**, 318 (1994).
[10] L. Boström *et al.*, Phys. Scr. **2**, 65 (1970).
[11] G. L. Catchen, Hyperfine Interact. **88**, 1 (1994).
[12] B. Lindgren, Hyperfine Interact. C **1**, 613 (1996); (private communication).
[13] M. E. Lines and A. M. Glass, *Principles and Applications of Ferroelectrics and Related Materials* (Clarendon, Oxford, 1977); G. L. Catchen, W. E. Evenson, and D. Allred, Phys. Rev. B **54**, R3679 (1996).
[14] M. Eibschütz, S. Shtrikman, and D. Treves, Phys. Rev. **156**, 562 (1967).
[15] G. L. Catchen, S. J. Wukitch, D. M. Spaar, and M. Blaszkiewicz, Phys. Rev. B **42**, 1885 (1990).
[16] F. Moussa, M. Hennion, J. Rodriguez-Carvajal, H. Moudden, L. Pinsard, and A. Recolevschi, Phys. Rev. B **54**, 15 149 (1996).